Performance Analysis of Compact Antenna Arrays with MRC in Correlated Nakagami Fading Channels

Jianxia Luo, *Student Member, IEEE*, James R. Zeidler, *Fellow, IEEE*, and Stephen McLaughlin, *Member, IEEE*

***Abstract*—This paper presents the average error probability performance of a compact space diversity receiver for the reception of binary coherent and noncoherent modulation signals through a correlated Nakagami fading channel. Analytical expressions of the average bit error rate (BER) are derived as a function of the covariance matrix of the multipath component signals at the antenna elements. Closed-form expressions for the spatial cross-correlation are obtained under a Gaussian angular power profile assumption, taking account of the mutual coupling between antenna elements. The effects of antenna array configuration (geometry and electromagnetic coupling) and the operating environment (fading, angular spread, mean angle-of-arrival) on the BER performance are illustrated.**

***Index Terms*—Bit error rate (BER), compact antenna array, correlated Nakagami fading channels, mutual coupling, space diversity.**

I. Introduction

SPATIAL diversity techniques have been shown to provide an effective means to combat multipath fading and to mitigate cochannel interference in mobile wireless communication systems. However, the diversity gain is reduced by the correlation of the fading signals between the antenna branches. The use of a compact space diversity receiver in handheld phones and portable terminals ensures that the received signals will be at least partially correlated, since the compact nature of the array will place antenna elements with a separation of a fraction of a wavelength. The performance of these compact receiver arrays thus requires an analysis that addresses the effects of correlated multipath arrivals at the elements of the receiver array.

The effect of correlated fading on the performance of a diversity combining receiver has received a great deal of research interest. Many works [3]–[8], [27] used the Rayleigh distribution to model the fading statistics of the channel. Recently, there has been a continued interest in modeling various propagation channels with the Nakagami-m distribution [1], which includes Rayleigh as a special case for $m = 1$. It is also a good approximation for Rice distribution when $m > 1$ [2]. In the literature, early studies on the performance of a maximal-ratio combiner (MRC) in the correlated Nakagami environment concentrated either on dual-branch diversity [12] or on arbitrary diversity order with simple correlation models (such as equal correlation and exponential correlation) [14].

In general, the cross-correlation between the signals received by antenna elements can take on any arbitrary symmetrical structure, since the cross-correlation depends not only on the antenna array configuration but also on the operating environment, e.g., the direction of incoming multipath waves and their angular spread. Closed-form expressions for the error probability in Nakagami fading channels with a general branch correlations were obtained in [15], taking into account the average branch signal-to-noise ratio (SNR) imbalance. Though the results are general for any diversity order and arbitrary branch correlation model (with the only limitation being the identical branch fading), the effect of antenna spacing and the operating environment on bit error rate (BER) performance can not be evaluated from [15], due to the lack of general expression of the spatial cross-correlation coefficient. Moreover, the average BER expression for coherent modulation contains an integral with infinite limits, which usually is not preferred from a computational standpoint [11].

More recently, [16] also addressed the same problem for coherent binary phase-shift keying (PSK) and frequency-shift keying (FSK) modulation. For the integer m, the result is expressed in the double summation form, but the coefficients in the partial sum representation involve the calculation of higher order differentiation of a product function. For the noninteger m, the solution is given in the form of a one-fold integral with infinite limits. The general results were used to analyze two antenna configurations commonly used in base stations with specified branch covariance matrix, leading to many interesting findings for system designs. The techniques developed in [15] and [16] both required that the covariance matrix be known before the average BER can be computed. This is convenient for the analysis of experimental data where the covariance matrix is explicitly measured from data, but it is not readily applied to the theoretical description of the array performance. This is because the correlation between the Nakagami faded amplitudes of the branch signals is very difficult to obtain in terms of the array configuration and the operating environment, even with the simple scattering model assumption.

In this paper, the analytical expressions for the average BER of an arbitrary order space diversity receiver are derived as functions of the covariance matrix of the multipath component signals at the antenna elements. We will show that the envelope of the received signal at each branch of the antenna array can be

Manuscript received November 15, 1999; revised June 26, 2000.

J. Luo is with the Electrical and Computer Engineering Department, University of California, San Diego, La Jolla, CA 92093-0407 USA and Hughes Network Systems, Inc., San Diego, CA 92121 USA (e-mail: jluo@ucsd.edu).

J. R. Zeidler is with the Electrical and Computer Engineering Department, University of California, San Diego, La Jolla, CA 92093-0407 USA and the Space and Naval Warfare Systems Center, San Diego, CA 92152-5001 USA (e-mail: zeidler@nosc.mil).

S. McLaughlin is with the Department of Electronics and Electrical Engineering, University of Edinburgh, Scotland EH9 3JL, U.K. (e-mail: sml@ee.ed.ac.uk).

Publisher Item Identifier S 0018-9545(01)01226-9.

expressed as the norm of an m-dimensional complex random vector, where m is the fading parameter of the Nakagami-m distribution. Each element of this m-dimensional random vector is orthogonal to the others and has a Rayleigh-distributed envelope. In this way, we can include the array configuration and effects of the operating environment in the performance assessment, since only the correlation between Gaussian component waves is required in the average BER expressions.

In addition, when antenna elements are placed very close (in terms of wavelength), they will reradiate the incident electromagnetic field, causing electromagnetic coupling between antenna elements. We will apply the classical "pattern multiplication" approach to an omnidirectional dipole or monopole antenna. This allows the received signal to be considered as a signal without mutual coupling multiplied by the array admittance matrix. Then, we can further extend the results of [7] and [8] in the flat Rayleigh fading channel to the Nakagami fading case.

The remainder of this paper is organized as follows. Section II describes the correlated Nakagami fading channel model and then analyzes the error performance for coherent and noncoherent modulation schemes. Closed-form expressions of the spatial cross-correlation of the underlying Rayleigh process are derived in Section III. Section IV addresses the effect of mutual coupling on spatial correlation. In Section V, we present numerical examples to illustrate the effects of various parameters on the BER performance. We offer some concluding remarks in Section VI.

II. Correlated Nakagami Channel

A. Channel Model

Consider an M-branch diversity receiver. The received baseband signal on kth branch can be written as

$$r_k(t) = s(t) \cdot A_k e^{j\phi_k} + n_k(t), \qquad k = 1, 2, \ldots, M \quad (1)$$

where $s(t)$ is the transmitted signal and $n_k(t)$ is independently identically distributed white Gaussian noise with zero mean and one-side spectral density N_0. The phase ϕ_k is uniformly distributed over the range [0, 2π). A_k is a Nakagami distributed signal envelope with a probability distribution function (pdf) given in [1]

$$p_{A_k}(A_k) = \frac{2}{\Gamma(m_k)} \cdot \left(\frac{m_k}{\Omega_k}\right)^{m_k} \cdot A_k^{2m_k-1} \cdot e^{-(m_k/\Omega_k)A_k^2}, \quad k = 1, 2, \ldots, M \quad (2)$$

where

$\Gamma(\cdot)$ Gamma function;
$\Omega_k = \overline{A_k^2}$ average power on kth branch;
m_k fading parameter, which must satisfy $m_k \geq 1/2$, describing the fading severity.

The smaller that m_k is, the more severe fading that occurs, with special cases $m_k = 1$ and $m_k = 1/2$ corresponding to the Rayleigh distribution and the one-sided Gaussian distribution, respectively.

Although the Nakagami-m distribution was originally developed in an empirical manner, based on field measurements, mathematically it is closely related to the χ-distribution with ν degrees of freedom. The pdf of the χ-distribution is given as [22]

$$p_{X_v}(x) = \frac{2}{(2\sigma^2)^{(v/2)} \cdot \Gamma(v/2)} \cdot e^{-x^2/2\sigma^2} \cdot x^{v-1}, \quad x > 0, \quad v > 0. \quad (3)$$

Substituting $m = v/2$ and $m/\Omega = 1/2\sigma^2$ into (3), we obtain an expression of the same form as the Nakagami-m pdf (2). It is straightforward to prove that the χ-distribution pdf is unimodal [22], and that the mode is at $\sqrt{v-1}\sigma$ for $\nu \geq 1$ and at the origin if $\nu < 1$ (this can be easily verified from the m-distribution pdf curves [1, Fig. 2.2]). Therefore, Nakagami-m distribution ($m \geq 1/2$) is equivalent to the central χ-distribution for $\nu \geq 1$. For m being a half-integer or integer, we can view a Nakagami random variable as the square root of the sum of squares of $2m$ independent Gaussian random variables. Then, m has the same interpretation as the degrees of freedom: as m increases, the number of Gaussian random variables added together increases, and the possibility of deep fades decreases.

In the mobile radio environment, it is reasonable to suppose that the received signal on the kth branch is superimposed by a large number of multipath signals. All component signals can be treated as m independent groups: in each group, there are n_j ($j = 1, \ldots, m$) unresolvable "subpath" signals r_k^{j,n_j}, which have almost identical amplitude and phase. The sum of these "subpath" signals in each group forms the jth "resolved" multipath component signal, i.e.,

$$r_k^{(j)} = \sum_{\{n_j\}} r_k^{j,n_j} = R_k^{(j)} \cdot e^{j\zeta_k} = x_k^{(j)} + iy_k^{(j)}, \quad j = 1, 2, \ldots, m_k. \quad (4)$$

Assuming that the set of n_j is large, then by invoking the central limit theorem, both $x_k^{(j)}$ and $y_k^{(j)}$ can be well approximated by independent Gaussian distributed random variables $N(0, \sigma^2)$; thus the amplitude $R_k^{(j)}$ is Rayleigh distributed. The received signal power on kth branch can be expressed as

$$A_k^2 = \sum_{j=1}^{m_k} \left| x_k^{(j)} + i \cdot y_k^{(j)} \right|^2 \equiv \langle \underline{r_k}, \underline{r_k} \rangle^2 \quad (5)$$

where

$\underline{r_k}$ $(r_k^{(1)} r_k^{(2)} \cdots r_k^{(m)})^T$;
$\langle \cdot \rangle$ the Euclidean norm;
$\overline{A_k}$ $2m_k\sigma^2$ from the independence of Gaussian components.

Assuming flat fading and perfect knowledge of the channel, the weighting factor in an MRC is $w_k = (A_k e^{j\phi_k})^*$, and thus the instantaneous SNR γ at the output of the MRC is given by [19]

$$\gamma = \frac{E_s}{N_0} \sum_{k=1}^{M} A_k^2 = \sum_{k=1}^{M} \gamma_k \quad (6)$$

where Es/N_0 is the ratio of the symbol energy to the Gaussian noise spectral density. The instantaneous input SNR per symbol for each branch is defined as $\gamma_k = (E_s/N_0) \cdot A_k^2$.

It is well known that the marginal pdf of γ_k follows the Gamma distribution

$$p_{\gamma_k}(\gamma_k) = \frac{m^m}{\Gamma(m)} \cdot \frac{\gamma_k^{m-1}}{(\overline{\gamma_k})^m} \cdot e^{-m(\gamma_k/\overline{\gamma_k})}, \quad k = 1, 2, \ldots, M \tag{7}$$

where $\overline{\gamma_k} = E[\gamma_k]$ is the average input SNR per symbol for the kth branch.

In the following derivation, we assume that each branch experiences the same extent of fading, i.e., $m_k = m$ for $k = 1, 2, \ldots, M$; thus $\underline{r_k}$s have the same dimension. Considering that the elements are placed very close, this is a more valid assumption in the compact array case than in a well-separated antenna array case, such as in base stations. In addition, the average signal power and the noise power density are assumed to be identical for each branch, so each γ_k has an identical marginal probability density function given by (7).

B. BER Performance

The average error probability in the presence of fading is obtained by averaging the conditional error probability over the pdf of γ, i.e.,

$$P_e = \int_0^\infty P(e|\gamma) \cdot p(\gamma) \cdot d\gamma. \tag{8}$$

In this paper, we will use some well-known conditional error probability expressions for coherent and noncoherent modulation schemes. To derive $p(\gamma)$, we follow the steps outlined in [19]: first find the characteristic function of γ, Φ_γ, then perform the inverse Fourier transform to obtain $p(\gamma)$.

Let $\underline{X_p}$ be a $2M$-dimensional Gaussian random vector to represent jth component signal vector

$$\underline{X_p} = [x_1, y_1, x_2, y_2, \ldots, x_M, y_M]$$

where $\{x_k, y_k\}$ are quadrature components received on the kth antenna branch.

X_p has a joint $2M$-variate Gaussian pdf [21] with zero-mean and covariance matrix Σ

$$\Sigma = \sigma^2 \cdot \begin{bmatrix} a_1 & 0 & b_{12} & \beta_{12} & \cdots & b_{1M} & \beta_{1M} \\ 0 & a_1 & \beta_{21} & b_{21} & \cdots & \beta_{M1} & b_{M1} \\ b_{21} & \beta_{21} & a_2 & 0 & \cdots & b_{2M} & \beta_{2M} \\ \beta_{12} & b_{12} & 0 & a_2 & \cdots & \beta_{M2} & b_{M2} \\ \vdots & \vdots & \vdots & \vdots & \ddots & \vdots & \vdots \\ b_{M1} & \beta_{M1} & b_{M2} & \beta_{M2} & \cdots & a_M & 0 \\ \beta_{1M} & b_{1M} & \beta_{2M} & b_{2M} & \cdots & 0 & a_M \end{bmatrix}_{2M \times 2M} \tag{9}$$

where $\sigma^2 = E(x_k x_k) = E(y_k y_k)$, $a_k = E(x_k^2)/\sigma^2 = 1$

$$b_{kl} = E(x_k x_l)/\sigma^2 = b_{lk} \tag{10a}$$

$$\beta_{kl} = E(x_k y_l)/\sigma^2 = -\beta_{lk} \tag{10b}$$

and b_{kl} and β_{kl} are referred as component correlation coefficients.

In general, for $\underline{X_p} \sim N(\underline{0}, \Sigma)$, the central Wishart distribution with covariance Σ and m degrees of freedom is defined as [21]

$$\underline{S} = \sum_{p=1}^{m} \underline{X_p} \cdot \underline{X_p}^T \sim W(\Sigma, m) \tag{11}$$

and S has the following characteristic function [21]:

$$\Phi_S = E\left[\exp(i \cdot \mathrm{tr}\,(\underline{S} \cdot \underline{T})\right] = \frac{1}{|I_{2M} - 2i \cdot \underline{T}\Sigma|^{m/2}} \tag{12}$$

where $\underline{T} = (t_{ij})_{i,\,j=1,\,2\ldots,\,2M}$, with $t_{ij} = t_{ji}$. I_{2M} is the $2M \times 2M$ identity matrix and $|F|$ indicates the determinant of the matrix F.

Setting the nondiagonal elements of T equal to zero and $t_{ii} = t$, $i = 1, 2, \ldots, 2M$, the multivariate gamma distribution is viewed as a special case of Wishart distribution

$$\begin{aligned} \Phi_S &= E\left[\exp(i \cdot \mathrm{tr}\,(\underline{S} \cdot \underline{T})\right] = E\left[\exp\left(i \cdot \sum_{k=1}^{M} A_k^2 t\right)\right] \\ &= E\left[\exp\left(\frac{i}{E_s/N_0} \cdot \sum_{k=1}^{M} \gamma_k t\right)\right] = E\left[\exp\left(\frac{i \cdot t}{E_s/N_0} \cdot \gamma\right)\right]. \end{aligned} \tag{13}$$

Using the variable substitution $w = t/(E_s/N_0)$ and applying the property of the positive definite matrix [3]

$$|I_{2M} + z\Sigma|^{-1/2} = |I_M + z\Delta|^{-1} \tag{14}$$

we obtain the general expression for the characteristic function of γ, i.e.,

$$\Phi_\gamma(w) = \left|I_{2M} - iw\frac{2E_s}{N_0}\Sigma\right|^{-m/2} = \left|I_M - iw\frac{\overline{\gamma}}{m}\Lambda\right|^{-m} \tag{15}$$

where $\overline{\gamma} = (E_s/N_0) \cdot \overline{A_k^2} = (E_s/N_0) \cdot (2m\sigma^2)$ and

$$\Delta = \sigma^2 \begin{bmatrix} a_1 & B_{12}^* & B_{13}^* & \cdots & B_{1M}^* \\ B_{12} & a_2 & B_{23}^* & \cdots & B_{2M}^* \\ B_{13} & B_{23} & a_3 & \cdots & B_{3M}^* \\ \vdots & \vdots & \vdots & \ddots & \vdots \\ B_{1M} & B_{2M} & B_{3M} & \cdots & a_M \end{bmatrix}_{M \times M} \equiv \sigma^2 \Lambda \tag{16}$$

where $B_{kl} = b_{kl} + i\beta_{kl}$ and the asterisk indicates the complex conjugate.

Equation (15) will be used to determine the BER performance in Section II-C. It is worthwhile to mention that although the characteristic function (15) has a very similar form as the moment generating function [15, eq. (11)]. Each element of Λ is the complex component correlation coefficient between the complex Gaussian component waves received at any two antennas, instead of the square root of power correlation coefficients in [15]. To be precise, the complex component correlation considered in this paper is the correlation between two field components (R_F in [27]), which allows the component correlation to be evaluated in terms of the antenna spacing, mean angle-of-arrival and angular spread, etc. The correlation utilized in [15]

representing the correlation between the instantaneous power of two received signals (R_{A^2} in [27]) is more convenient for the analysis of experimental data, where the correlation of the signal power can be easily measured from field data.

In the above derivations, we initially assume that m is an integer, while in the Appendix, we will show that the characteristic function (15) is also valid for any positive real value $m \geq 1/2$.

C. Binary PSK/FSK Reception

In the following, we apply the general expression to several coherent and noncoherent modulation schemes.

1) DBPSK and NBFSK: The conditional BER for differential binary phase-shift keying (DBPSK) and noncoherent binary orthogonal frequency-shift keying (NBFSK) is given in [19] as

$$P(e|\gamma) = \tfrac{1}{2}\exp(-a\gamma) \tag{17}$$

where a is the modulation constant, i.e., $a = 1/2$ corresponds to NBFSK and $a = 1$ is for BDPSK.

Substituting (15) into (8), we readily obtain the average BER expression, i.e.,

$$\begin{aligned}\overline{P}_{eN} &= \frac{1}{2}\int_0^\infty e^{-a\gamma}p(\gamma)\,d\gamma = \frac{1}{2}\,\Phi_\gamma(t)|_{it=-a} \\ &= \frac{1}{2}\left|I_M + \frac{a\overline{\gamma}}{m}\,\Lambda\right|^{-m}. \end{aligned}\tag{18}$$

Thus, given the diversity order M, $\overline{P_{eN}}$ can easily be expressed as the polynomial of the component correlation coefficients between antenna elements. For a dual diversity receiver, (18) agrees with the general expression in [14] for $M = 2$, the noncoherent case.

2) CBPSK and CBFSK: The conditional error probability for coherent binary phase-shift keying (CBPSK) and coherent binary frequency-shift keying (CBFSK) is given by [19]

$$P(e|\gamma) = Q\left(\sqrt{2a\gamma}\right) \tag{19}$$

where $a = 1/2$ and $a = 1$ correspond to CBFSK and CBPSK, respectively, and $Q(x)$ is the Gaussian Q-function. Using the alternate representation of $Q(x)$ given in [11]

$$Q(x) = \frac{1}{\pi}\int_0^{\pi/2}\exp\left(-\frac{x^2}{2\sin^2\vartheta}\right)d\vartheta, \qquad x \geq 0. \tag{20}$$

The average BER can then be written as

$$\begin{aligned}\overline{P}_{eC} &= \frac{1}{\pi}\int_0^\infty\int_0^{\pi/2}\exp\left(-\frac{a\gamma}{\sin^2\vartheta}\right)d\vartheta\cdot p(\gamma)\,d\gamma \\ &= \frac{1}{\pi}\int_0^{\pi/2}\Phi_\gamma(t)\Big|_{it=-a/\sin^2\theta}\,d\vartheta \\ &\equiv \frac{1}{\pi}\int_0^{\pi/2}\left|I_M + \frac{a\overline{\gamma}}{m\cdot\sin^2\vartheta}\,\Lambda\right|^{-m}d\vartheta. \end{aligned}\tag{21}$$

The above expression only requires an integral with finite limits, and it is easy and accurate to use numerical integration tools in Maple or Matlab software package to evaluate the results. By setting $M = 2$, the average BER for the dual diversity receiver can be obtained

$$\begin{aligned}\overline{P}_{eC} = \frac{1}{\pi}\int_0^{\pi/2}\Bigg\{&\left(1 + \frac{a}{\sin^2\vartheta}\cdot\frac{\overline{\gamma}}{m}\right)^2 \\ &- \left(\frac{a}{\sin^2\vartheta}\cdot\frac{\overline{\gamma}}{m}\right)^2\cdot|B_{12}|^2\Bigg\}^{-m}d\vartheta \end{aligned}\tag{22}$$

and for the case of independent branches, (22) reduces to

$$\overline{P}_{eC} = \frac{1}{\pi}\int_0^{\pi/2}\left(1 + \frac{a}{\sin^2\vartheta}\cdot\frac{\overline{\gamma}}{m}\right)^{-2m}d\vartheta. \tag{23}$$

It is noted that (23) is equivalent to that in [14], which is expressed in terms of the Gaussian hypergeometric function ${}_2F_1(\cdot,\cdot;\cdot;\cdot)$.

III. Spatial Correlation Coefficients

The spatial diversity gain of combating multipath fading of the desired signal is reduced by the correlation of the received signal between the antenna branches. However, studies reported in [4] and [5] on the effect of fading correlations have shown that the degradation in performance can be small even for correlations as high as 0.7. To better understand the effect of physical configuration of the antenna array and operating environment parameters on the performance, and consequently help design suitable compact arrays in different applications, it is important to provide cross-correlation analyses with realistic assumptions for the different environments. In this section, we will extend the theoretical analysis in [4] by assuming a Gaussian distributed spatial angle of arrival (AOA). The measurement data [9] for GSM systems in rural and suburban environment confirms that this is a more realistic model than the uniform AOA distribution [4]. Previous analyses in [5] and [8] also used the Gaussian AOA model.

In the following analysis, the receiver antenna array is modeled as a linear array of M vertical omnidirectional antennas, e.g., dipoles or monopoles, with the horizontal separation d between antenna elements. Fig. 1 shows the geometrical model of the antenna array, where φ_0 is the mean direction of arrival and σ_φ is the angular spread.

The azimuthal AOA has a Gaussian pdf

$$p(\varphi) = \frac{\kappa}{\sqrt{2\pi}\,\sigma_\varphi}\,e^{-(\varphi-\varphi_0)^2/2\sigma_\varphi^2}, \qquad \varphi \in [-\pi+\varphi_0,\,\pi+\varphi_0] \tag{24}$$

where κ is the normalization factor to make $p(\varphi)$ a physical density function, i.e.,

$$\kappa = 1\Big/\operatorname{erf}\left(\frac{\pi}{\sqrt{2}\sigma_\varphi}\right) \tag{25}$$

where $\operatorname{erf}(x) = (2/\sqrt{\pi})\int_0^x e^{-t^2}\,dt$ is the error function. Note that when the angular spread is small, κ is almost equal to unity.

For the BER expressions we obtained in Section II, we are particularly interested in the complex cross-correlation [20] between the jth complex Gaussian component signals received at the kth and lth antenna

$$\begin{aligned}c_{kl} &= \tfrac{1}{2}E\left[r_k^{(j)}(t)\cdot r_l^{(j)*}(t)\right] \\ &= E\left[x_k^{(j)}(t)\cdot x_l^{(j)}(t)\right] + i\cdot E\left[x_k^{(j)}(t)\cdot y_l^{(j)}(t)\right]. \end{aligned}\tag{26}$$

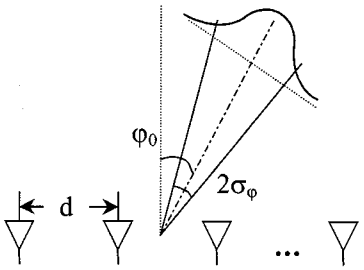

Fig. 1. Geometry model of linear antenna array.

Assuming that the fading of the amplitude and phase are statistically independent, and that $\{x_k^{(j)}(t),\, y_k^{(j)}(t)\}$ are independent of j (from this point on, we will drop superscript j for notational clarity), we obtain the normalized cross-correlation coefficient

$$B_{kl} = \frac{1}{\sqrt{P_k P_l}} \cdot \int_{\phi_0-\pi}^{\phi_0+\pi} r_k \cdot r_l^* \cdot p(\varphi)\, d\varphi \equiv b_{kl} + i\beta_{kl} \quad (27)$$

where b_{kl} and β_{kl}, $k, l = 1, \ldots, M$, are the normalized component correlation coefficients defined as in (10a) and (10b), and P_k is the average power of a component signal received on the kth branch, defined as

$$P_k = \int_{\varphi_0-\pi}^{\varphi_0+\pi} |r_k(\varphi)|^2 \cdot p(\varphi)\, d\varphi, \qquad k = 1, 2, \ldots, M. \quad (28)$$

Assuming a plane wave arriving in the direction of φ, the relative phase delay of the kth antenna is given as

$$\tau_k = 2\pi \frac{kd}{\lambda} \cdot \sin\varphi. \quad (29)$$

Then

$$B_{kl} = \int_{\phi_0-\pi}^{\phi_0+\pi} e^{i2\pi(((k-l)d)/\lambda)\sin\varphi} \cdot p(\varphi)\, d\varphi. \quad (30)$$

Letting $z = 2\pi(d/\lambda)$, we obtain

$$b_{kl} = \int_{\phi_0-\pi}^{\phi_0+\pi} \cos[z(k-l)\sin\varphi] \cdot p(\varphi)\, d\varphi \quad (31)$$

$$\beta_{kl} = \int_{\phi_0-\pi}^{\phi_0+\pi} \sin[z(k-l)\sin\varphi] \cdot p(\varphi)\, d\varphi. \quad (32)$$

Following the same procedure outlined in [4, Appendix], we obtain the following closed-form expressions for the component correlation coefficients:

$$b_{kl} = J_0[(k-l)z] + 2\kappa \sum_{m=1}^{\infty} J_{2m}[(k-l)z] \cdot \cos(2m\varphi_0) \cdot e^{-2m^2\sigma_\varphi^2} \cdot \Re e\left[\operatorname{erf}\left(\frac{\pi + i2m\sigma_\varphi^2}{\sqrt{2}\sigma_\varphi}\right)\right] \quad (33)$$

$$\beta_{kl} = 2\kappa \sum_{m=0}^{\infty} J_{2m+1}[(k-l)z] \cdot \sin[(2m+1)\varphi_0] \cdot e^{-(2m+1)^2\sigma_\varphi^2/2} \cdot \Re e\left[\operatorname{erf}\left(\frac{\pi + i(2m+1)\sigma_\varphi^2}{\sqrt{2}\sigma_\varphi}\right)\right] \quad (34)$$

where $\Re e(x)$ is the real part of x and $\operatorname{erf}(a+ib)$ is the complex-input error function [24], which can be numerically evaluated using Maple. Expressed in more compact form, (33) and (34) are, in essence, very similar to expressions obtained in [10], which only integrates over $[-\pi/2+\varphi_0, \pi/2+\varphi_0]$. For the numerical evaluation, the summation over 30 terms is enough for accuracy to six digits after the decimal point.

In addition, the cross-correlation of the envelopes of two signals ρ_{env} can be approximated [3] by the squared modulus of the complex component cross-correlation $|B_{kl}|^2$, referred to as the power correlation coefficient, i.e.,

$$\rho_{\text{env}} \approx \frac{1}{P_k P_l}\left|\int_{\varphi_0-\pi}^{\varphi_0+\pi} r_k(\varphi) \cdot r_l^*(\varphi) \cdot p(\varphi)\, d\varphi\right|^2 = |b_{kl} + i\beta_{kl}|^2 = |B_{kl}|^2. \quad (35)$$

Thus, ρ_{env} can be readily evaluated, given the component cross-correlation expression.

IV. Mutual Coupling Effect

In above analysis, it was assumed that the receiving antenna array only passively sampled the incident fields spatially. But the elements of the array, in reality, not only spatially sample but also reradiate the incident fields causing the mutual coupling between the array elements. Previous results in [26] and [8] indicate that for small antenna spacing ($d < 0.5\lambda$), the mutual coupling effect is significant, so mutual coupling (MC) should be taken into account in the performance analysis of a compact receiver.

Considering the M-element array as an $M+1$ terminal linear bilateral network responding to an outside source, and assuming that each antenna is terminated with a known load impedance Z_L, [26] gives the following relationship between two sets of received voltage V_k and S_k with and without mutual coupling, respectively:

$$\begin{bmatrix} 1+\frac{Z_{11}}{Z_L} & \frac{Z_{12}}{Z_L} & \cdots & \frac{Z_{1M}}{Z_L} \\ \frac{Z_{21}}{Z_L} & 1+\frac{Z_{22}}{Z_L} & \cdots & \frac{Z_{2M}}{Z_L} \\ \vdots & \vdots & \ddots & \vdots \\ \frac{Z_{M1}}{Z_L} & \frac{Z_{M2}}{Z_L} & \cdots & 1+\frac{Z_{MM}}{Z_L} \end{bmatrix} \cdot \begin{bmatrix} V_1 \\ V_2 \\ \vdots \\ V_M \end{bmatrix} = \begin{bmatrix} S_1 \\ S_2 \\ \vdots \\ S_M \end{bmatrix}. \quad (36)$$

Written in the matrix form

$$ZV = S$$

where Z_{kk} is the self-impedance and Z_{kl} is the mutual impedance between the kth and lth antennas. Note that $Z_{kl} = Z_{lk}$ from the reciprocity theorem [25].

Since Z is always nonsingular, the element output voltages (which will be used as the input signals to the MRC combiner) can be obtained as

$$V = Z^{-1}S \tag{37}$$

where Z^{-1} is also referred to as the array admittance matrix, depending only on the self-impedance and mutual impedance normalized by the load impedance. It acts like a transforming matrix, transforming the open circuit element voltages to the terminal voltages.

In this paper, as a simple example for illustration, we will apply the classical "pattern multiplication" method to a dual-branch uniform linear array with each element as a half-wave dipole or monopole, for which [25] provides the closed-form expressions of the self-impedance and mutual impedance. For this case, the relative pattern attributable to the individual elements can be assumed to be identical; the "element pattern" often closely matches that of an isolated element located in free space, and then can be factored out of the complete array pattern expression. For a two-element linear dipole or monopole array, this implies that the coupling matrix is

$$Z = \begin{bmatrix} 1 + \dfrac{Z_{11}}{Z_L} & \dfrac{Z_{12}}{Z_L} \\ \dfrac{Z_{21}}{Z_L} & 1 + \dfrac{Z_{22}}{Z_L} \end{bmatrix} \tag{38}$$

and the source vector obtained without coupling can be written as

$$S(\varphi) = \begin{bmatrix} g_1(\varphi_1, \theta_1) \cdot 1 \\ g_2(\varphi_2, \theta_2) \cdot e^{i2\pi(d/\lambda)\sin\varphi} \end{bmatrix} \tag{39}$$

where φ_k and θ_k are the azimuthual and elevation angle, respectively; $g_k(\varphi_k, \theta_k)$ is a vector function proportional to the electrical field and represents the radiation pattern of the identical antenna element. We restrict our interest to the horizontal plane $\theta_k = \pi/2$ only, and for omnidirectional antennas, $g_k(\varphi_k, (\pi/2)) \equiv 1$. With coupling, the corresponding source vector is

$$V(\varphi) = Z^{-1} \cdot S(\varphi). \tag{40}$$

Let $Z^{-1} = \begin{bmatrix} a & b \\ b & a \end{bmatrix}$; then we have

$$\begin{aligned} V(\varphi) &= \begin{bmatrix} V_1(\varphi) \\ V_2(\varphi) \end{bmatrix} = \begin{bmatrix} g(\varphi) \cdot (a + b \cdot e^{iz\sin\varphi}) \\ g(\varphi) \cdot (b + a \cdot e^{iz\sin\varphi}) \end{bmatrix} \\ &= \begin{bmatrix} a + b \cdot e^{iz\sin\varphi} \\ b + a \cdot e^{iz\sin\varphi} \end{bmatrix}. \end{aligned} \tag{41}$$

Substituting the expression of $V_k(\varphi)$ into (28), we obtain

$$\begin{aligned} P_1 &= \int_{\varphi_0-\pi}^{\varphi_0+\pi} \left(|a|^2 + |b|^2 + ab^* e^{-iz\sin\varphi} + ba^* e^{iz\sin\varphi}\right) \\ &\quad \cdot p(\varphi)\, d\varphi \\ &= |a|^2 + |b|^2 + ab^* \cdot \int_{\varphi_0-\pi}^{\varphi_0+\pi} e^{-iz\sin\varphi} \cdot p(\varphi)\, d\varphi \\ &\quad + ba^* \cdot \int_{\varphi_0-\pi}^{\varphi_0+\pi} e^{iz\sin\varphi} \cdot p(\varphi)\, d\varphi. \end{aligned} \tag{42}$$

Noticing that two integral terms in (42) are the same as in (30) with $k - l = 1$, we obtain

$$P_1 = |a|^2 + |b|^2 + 2b_{12} \cdot \Re e(ab^*) + 2\beta_{12} \cdot \mathrm{Im}(ab^*). \tag{43a}$$

Similarly, we have

$$P_2 = |a|^2 + |b|^2 + 2b_{12} \cdot \Re e(ab^*) - 2\beta_{12} \cdot \mathrm{Im}(ab^*). \tag{43b}$$

Substituting $V_k(\varphi)$ into (35), the normalized power correlation can be written as

$$\begin{aligned} |\rho_{12}|^2 = \frac{1}{P_1 P_2} \big| &(|a|^2 + |b|^2) \cdot b_{12} + 2 \cdot \Re e(ab^*) \\ &+ j \cdot (|a|^2 - |b|^2) \cdot \beta_{12} \big|^2. \end{aligned} \tag{44}$$

The theoretical calculation results in the next section show that this effect reduces the spatial correlation and improves BER performance, which provides additional motivation for applying the spatial diversity in compact handheld terminals.

V. Numerical Results

In this section, we present a series of numerical examples to illustrate the effects of the antenna configuration and the operating environment (i.e., fading, nominal AOA, angular spread, and mutual coupling) on spatial correlation coefficients and on the BER performance of the compact receiver in different Nakagami-m fading channels.

From (33) and (34), we know that the spatial correlation is a function of the antenna spacing, mean incident angle of multipath signal, and angular spread. Fig. 2 shows the power correlation coefficient versus antenna spacing for mean angle-of-arrival $\varphi_0 = 30°$ with various angular spreads. The plots obtained for the broadside ($\varphi_0 = 0°$) and end-fire ($\varphi_0 = 90°$) cases are similar to those in [10] and are not repeated here. It is apparent that increasing antenna separation between the antenna elements always reduces their correlation, and that the separation required for a given correlation coefficient decreases quickly as the angular spread increases.

Substituting the component correlation coefficients into the average BER expression (18) and (21), we will see how those parameters affect BER performance in a correlated Nakagami-m fading channel. In addition, we will use the diversity gain [18] (defined as the reduction in the average SNR of a diversity system that maintains the same BER at the receiver as a system without diversity) in the performance comparisons.

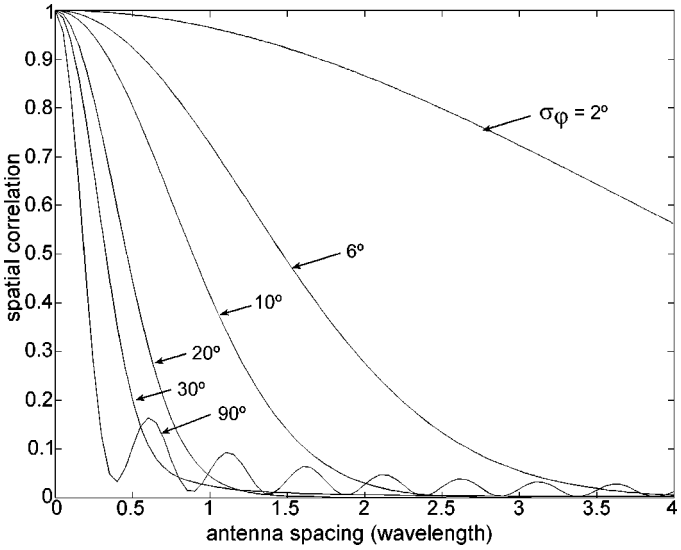

Fig. 2. Power correlation versus antenna spacing at $\varphi_0 = 30^\circ$ for different angular spread σ_φ.

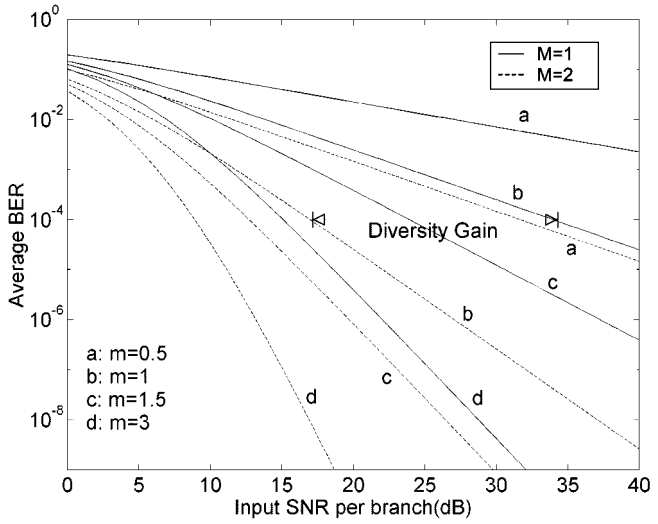

Fig. 3. BER comparison of dual diversity and no diversity in different m fading channels for CBPSK, with $d = (1/4)\lambda$, broadside, angular spread $\sigma_\varphi = 60^\circ$.

A. Influence of the Fading Parameter

Fig. 3 plots the average BER of a dual-diversity $(M = 2)$ MRC receiver versus the average input SNR per branch for CBPSK, with broadside receiving, antenna spacing 1/4λ, and fixed angular spread $\sigma_\varphi = 60^\circ$, in different fading channels. The cases for no diversity $(M = 1)$ are shown for comparison and to calculate the diversity gain. As expected, the average BER performance improves with increased fading parameter m; and in more severe fading channels, a larger diversity gain is obtained, making it possible to maintain reasonable system performance with a space diversity receiver, even in deep fades. For example, at $P_e = 10^{-2}$, the diversity gain is 16 dB for $m = 0.5$; it decreases to 7.4 dB for $m = 1$.

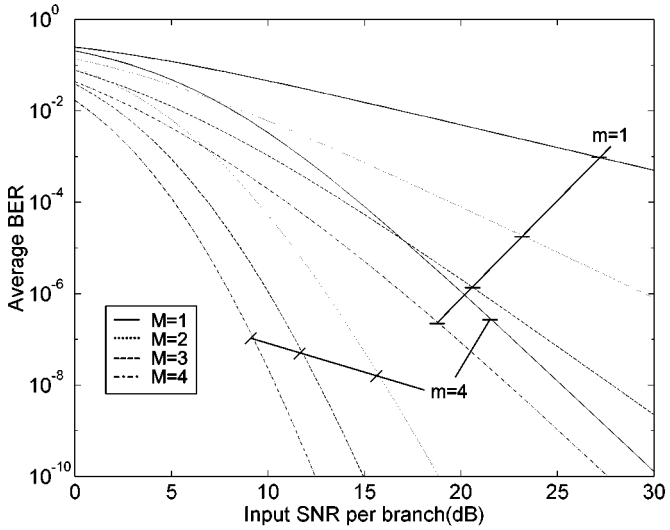

Fig. 4. Effect of diversity order in $m = 1$ and $m = 4$ fading channels, DBPSK, broadside, antenna spacing $d = (1/4)\lambda$, angular spread $\sigma_\varphi = 45^\circ$.

B. The Diversity Order

Fig. 4 shows the average BER of DBPSK for $M = 1, 2, 3, 4$ branches, broadside receiving, antenna spacing 1/4λ, and fixed angular spread $\sigma_\varphi = 45^\circ$ in $m = 1$ and $m = 4$ fading channels. We can see that the diversity gain obtained by increasing from $M = 1$ to $M = 2$ is dominant, which agrees with the conclusion for the Rayleigh fading channel [18]. It also shows that at large values of SNR, the BER curves become linear with the input branch SNR, and the asymptotic slope of $\log_{10} P_e$ versus $\log_{10}$ (input branch SNR) is $(-mM)$ [28]. As shown in Fig. 4, the curve for $m = 1$, $M = 4$ has the same slope as that for $m = 4$, $M = 1$. This means that the BER performance improvement for a small diversity order receiver in the severe fading channels is the most significant. However, the use of a large diversity order to improve the system performance is often restricted by the implementation complexity. In particular, for a compact receiver design, the dimension of the array is an extremely important constraint.

C. Effect of Antenna Spacing

Fig. 5 gives the variation of the BER versus the antenna spacing for dual diversity with broadside receiving, two typical angular spreads $\sigma_\varphi = 6^\circ$ and 60°, and fixed branch SNR $=$ 20 dB in $m = 0.8$ and $m = 1.5$ fading channels. A larger antenna spacing is needed to give better performance for a smaller angular spread, which can be explained by the very slow reduction of the spatial correlation for a small angular spread. Regardless of the angular spread, once the antenna spacing is increased beyond 2λ, the BER performance starts approaching its maximum achievable fading gain without further improvement. Thus, the lack of high angular spread (as in an outdoor rural environment) can be compensated for by increasing antenna separation. It should be noted that when the antenna spacing is decreased from 0.5λ to 0.1λ, the BER

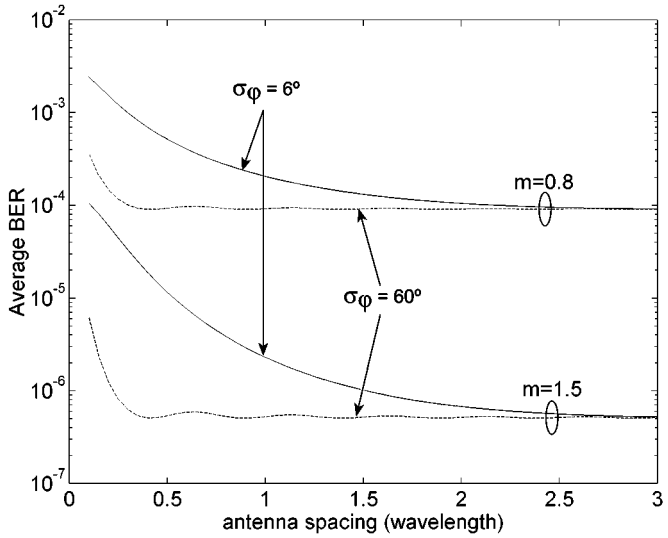

Fig. 5. Effect of antenna spacing, dual diversity, broadside, in $m = 0.8$ and $m = 1.5$ fading channels, with angular spread $\sigma_\varphi = 6^\circ$ and 60°, respectively.

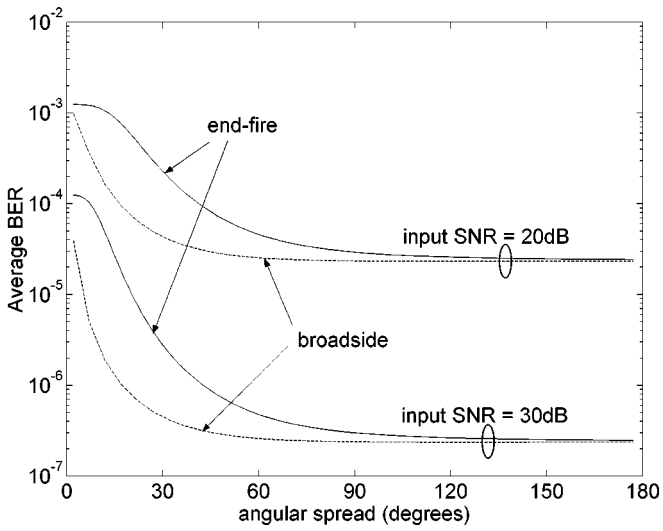

Fig. 6. BER versus angular spread with 1/4λ antenna separation in $m = 1$ Nakagami fading channel (Rayleigh).

increases by approximately five-fold and ten-fold for $m = 0.8$ and $m = 1.5$, respectively. However, to be more realistic, the effect of mutual coupling must be included for very small antenna separation. This will be addressed in Section V-F.

D. Sensitivity to the Angular Spread

Fig. 6 shows the BER versus the angular spread at fixed SNR and two extreme mean AOA cases in an $m = 1$ fading channel. For broadside, the average BER has a noticeable degradation when the angular spread is decreased below 25°; while for end-fire, there is a fast degradation as the angular spread decreases from 60°. Table I lists the dual-diversity gain at BER $= 10^{-3}$ and 10^{-5} for typical angular spreads in different fading channels.

We notice that for a given m and fixed mean AOA, the smallest decrease in diversity occurs in going from $|B_{kl}|^2 = 0.1$ to 0.3, and the largest gain decrease occurs in going from $|B_{kl}|^2 = 0.6$ to 0.9. This indicates that for small to medium correlation coefficients ($|B_{kl}|^2 < 0.6$), much of the diversity improvement can still be obtained [13]. Also, as the average SNR increases (the Pe decreases), the diversity gain increases and the deleterious effects of the correlation decrease.

TABLE I
DIVERSITY GAIN (dB) FOR DIFFERENT ANGULAR SPREAD

Angular spread		Power	Diversity gain at 10^{-3}			Diversity gain at 10^{-5}	
Broad-side	End-fire	correlation	m=1	m=2	m=4	m=2	m=4
6°	24°	0.9	9.5	4.8	3.4	7.6	4.0
13°	39°	0.6	12.6	6.8	4.2	10.4	5.6
21°	57°	0.3	13.8	7.4	4.8	11.4	6.6
90°	150°	0.1	14.2	7.6	5.0	12.1	6.8

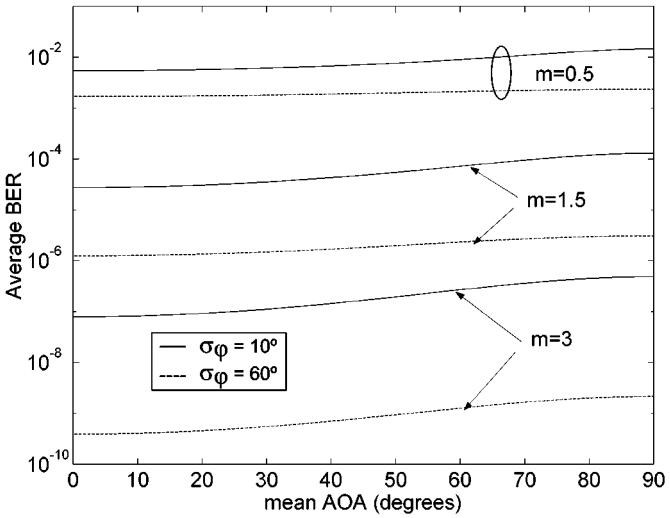

Fig. 7. Effect of AOA on average BER for different angular spread $\sigma_\varphi = 10^\circ$ and 60° and in different fading channels.

E. Sensitivity to the Mean AOA

Fig. 7 illustrates the sensitivity of BER performance to the mean AOA in different fading channels, with fixed branch SNR $= 20$ dB. We can see the gradual degradation when the mean AOA deviates from the broadside direction, but the degradation is relatively small in the whole range $[0, \pi/2]$ compared with the angular spread. Regardless of the angular spread, less severe fading channels create a large variation when the mean AOA changes from broadside to end-fire. For a severe fading channel, the large angular spread case is less sensitive to AOA, while for less severe fading channels ($m \geq 3$), small angular spread cases are less sensitive to AOA. Table II gives specific BER values at two extreme mean AOAs for different fading parameters and angular spreads, respectively. But since large angular spreads reduce the correlation more dramatically, sensitivity to the AOA in general will not cause much degradation.

A comparison among DBPSK, NBFSK, CBPSK, and CBFSK modulation is shown in Fig. 8 for a three-element linear antenna array with spacing $d = 0.25\lambda$, broadside receiving, and angular spread $\sigma_\varphi = 45^\circ$ at 20-dB fixed SNR in $m = 0.8$ and $m = 4$ fading channels. It is observed that the conventional 3-dB difference still exists for CBPSK and DBPSK over CBFSK and NBFSK, respectively. Fig. 8 also

TABLE II
VARIATION OF AVERAGE BER VERSUS FADING ENVIRONMENT

	σ_φ=10°		Variation	σ_φ=60°		Variation
BER	Broadside	End-fire	percentage	broadside	End-fire	percentage
m=0.5	0.0068	0.0156	229%	0.00146	0.00198	136%
m=1	4.38e-4	1.23e-3	280%	2.54e-5	4.58e-5	180%
m=1.5	4.41e-5	1.35e-4	306%	8.14e-7	1.95e-6	240%
m=3	1.49e-7	5.03e-7	337%	1.74e-10	9.1e-10	523%

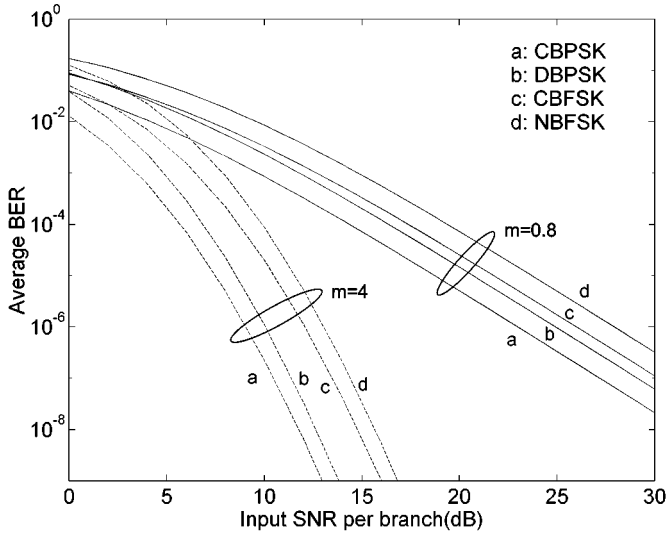

Fig. 8. Comparison among four modulation schemes with three-element antenna array, broadside receiving, and angular spread $\sigma_\varphi = 45^\circ$ in $m = 0.8$ and $m = 4$ fading channels.

serves as a validation of the BER expressions of various modulation schemes for a noninteger fading parameter m.

F. Mutual Coupling's Effect

Figs. 9 and 10 plot the power correlation versus the angular spread at different mean AOAs for the antenna spacing of 0.1λ and 0.5λ by numerically evaluating (44). It is evident that the effect of coupling can be neglected for antenna separation larger than half a wavelength. Fig. 11 shows the BER versus the antenna spacing for coherent BPSK, with fixed input branch SNR $= 20$ dB, broadside receiving, and angular spread $\sigma_\varphi = 60^\circ$ in $m = 0.8$, $m = 1$, and $m = 1.5$ Nakagami fading channels, respectively. It is clear that even for antenna separation $d = 0.1\lambda \sim 0.25\lambda$, the BER performance degradation is very small for large angular spreads. Therefore, applying spatial diversity on mobile terminals is feasible and can act as an important complement to adaptive arrays at the base stations, where the downlink currently constitutes the limit to potential capacity gains.

As shown in [8], these favorable results can be explained by the fact that the mutual coupling effect causes a pattern distortion and provides some pattern diversity. Thus, when the antenna spacing is extremely small, as in compact receiver cases, the pattern diversity effect dominates over the effect of the space diversity.

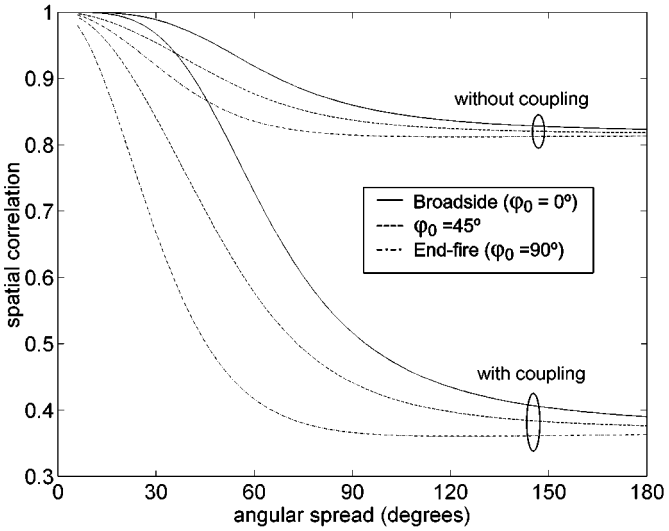

Fig. 9. Spatial correlation versus angular spread with different mean AOA and antenna spacing $d = 0.1\lambda$, with and without the presence of mutual coupling.

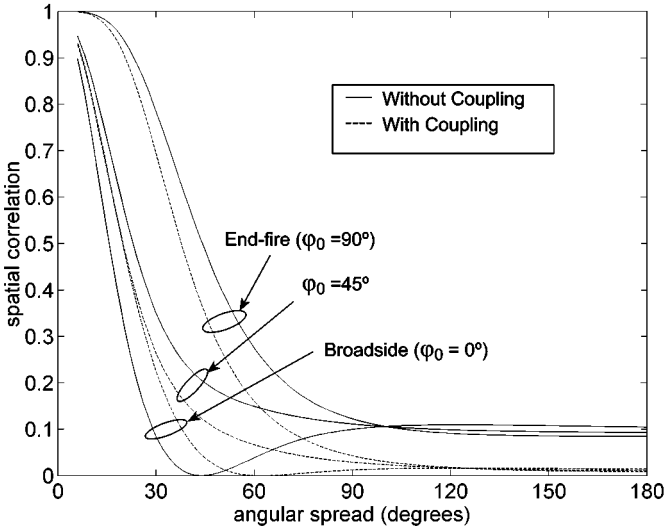

Fig. 10. Spatial correlation versus angular spread with different mean AOA and antenna spacing $d = 0.5\lambda$, with and without the presence of mutual coupling.

VI. CONCLUSION

This paper extends previous work [7], [8] investigating the effect of the spatial correlation on the average BER performance of a compact antenna array in Rayleigh fading to the Nakagami fading environment. The formulation does not require the knowledge of the spatial covariance matrices as in [15] and [16]. A new approach of viewing a Nakagami random variable as the norm of an m-dimension complex random vector was presented. Thus, the characteristic function of instantaneous SNR at the combiner's output can be expressed in terms of the cross-correlation matrix of the underlying Rayleigh processes. In the case of noncoherent binary PSK/FSK, the BER expression can be represented as a polynomial of the cross-correlation of Gaussian component signals, given the diversity order; for coherent reception, only a single finite-interval integration is required to evaluate the

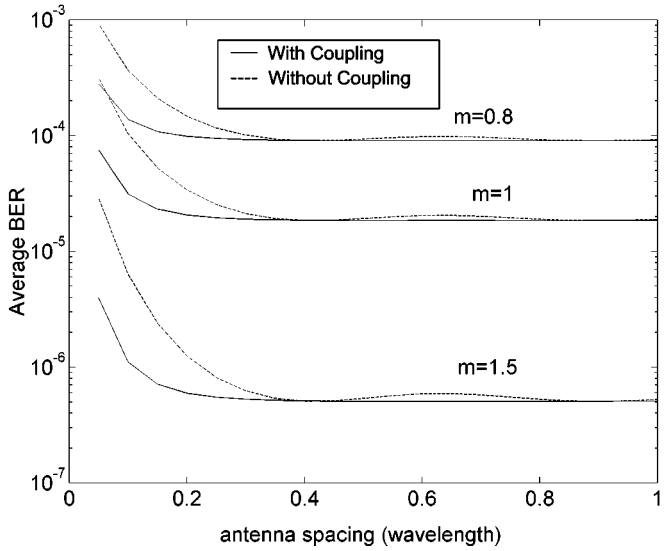

Fig. 11. BER versus antenna spacing in different fading channels, CBPSK, broadside receiving, and angular spread $\sigma_\varphi = 60^\circ$, with and without the presence of mutual coupling.

BER performance. A more realistic angular power profile, the Gaussian AOA distribution, is assumed in calculating spatial correlation coefficients. The numerical results clearly illustrate the sensitivity of the compact array to the fading parameter, diversity order, antenna spacing, mean AOA, and angular spread. For $d = 1/4\lambda$, broadside reception, there is negligible degradation as long as angular spread $\sigma_\varphi > 13^\circ$, while for the end-fire case, a larger angular spread ($\sigma_\varphi > 60^\circ$) is needed. In a severe fading channel, larger diversity gain is obtained for the same antenna spacing and angular spread.

In addition, mutual coupling was taken into account. Using simple dipole or monopole antennas as array elements in the analysis, the correlation coefficients decreased for $d = 0.1\lambda$, which is a favorable result for applying a spatial diversity receiver in handheld terminals.

APPENDIX

Recapitulating the proof in [17, Lemma 3], we can extend the characteristic function of γ (15) to the noninteger m. Since Λ is a normalized covariance matrix, it is at least positive semidefinite. Letting $g_i (i = 1, 2, \ldots, M)$ be the characteristic root of Λ, clearly g_i is nonnegative. Then

$$\Phi_\gamma(t) = \left[\prod_{i=1}^{M}\left(1 - it\frac{\overline{\gamma}}{m}\cdot g_i\right)\right]^{-m} = \left[\prod_{i=1}^{M}(1 - it\cdot d_i)\right]^{-m}$$

where $d_i = (\overline{\gamma}/m)\cdot g_i \geq 0$.

Let $\eta(t) = \prod_{i=1}^{M}(1 - it\cdot d_i)^{-1/2}$ be the characteristic function of the convolution of M Gamma distribution and $\Phi_\gamma(t)$ be the product of a $2m$ such characteristic function, each of which has the arithmetic mean, is infinitely divisible [17], and hence never vanishes. Therefore, the following operation is valid:

$$\eta(t) = \exp\left\{\frac{1}{2m}\log\Phi(t)\right\}.$$

Then

$$[\eta(t)]^{2m} = \exp\left\{\frac{p}{q}\log\Phi(t)\right\}$$

is a characteristic function for all integers $p, q > 0$. That is to say, if m is rational, the derived characteristic function is valid. Finally, from the continuity theorem [23], the conclusion can be extended to all positive values m.

It should be noted that in the mathematical expression of the characteristic function $\Phi_\gamma(t)$, m can be any positive, real number, and the restriction for $m \geq 1/2$ is due to the Nakagami-m distribution's communication application background.

ACKNOWLEDGMENT

The authors wish to thank the reviewers for their constructive suggestions.

REFERENCES

[1] M. Nakagami, "The m-distribution, a general formula of intensity distribution of rapid fading," in *Statistical Methods in Radio Wave Propagation*, W. G. Hoffman, Ed. Oxford, U.K.: Pergamon, 1960.
[2] W. R. Braun and U. Dersch, "A physical mobile radio channel model," *IEEE Trans. Veh. Technol.*, vol. 40, pp. 472–482, May 1991.
[3] J. N. Pierce and S. Stein, "Multiple diversity with nonindependent fading," *Proc. IRE*, vol. 48, pp. 89–104, Jan. 1960.
[4] J. Salz and J. Winters, "Effect of fading correlation on adaptive arrays in digital mobile radio," *IEEE Trans. Veh. Technol.*, vol. 43, pp. 1049–1057, Nov. 1994.
[5] F. Adachi *et al.*, "Crosscorrelation between the envelopes of 900 MHz signals received at a mobile radio base station site," *Proc. Inst. Elect. Eng.*, vol. 133, pp. 506–512, Oct. 1986.
[6] J.-F. Diouris and J. Zeidler, "Performance analysis of a compact array receiver for CDMA cellular communications," in *Proc. IEEE Military Commun. Conf.*, Oct. 1998, pp. 182–186.
[7] J. F. Diouris, J. Zeidler, and S. Buljore, "Space-path diversity in CDMA using a compact array," *Annales des Telecommun.*, vol. 53, no. 11–12, pp. 425–435, 1998.
[8] J. F. Diouris, K. Mahdjoubi, J. Zeidler, and J. Saillard, "The effect of coupling in a compact handset receiver," *Annales des Telecommun.*, vol. 54, no. 1–2, pp. 85–92, 1999.
[9] D. Aszetly, "On antenna arrays in mobile communication systems: Fast fading and GSM base station receiver algorithm," Ph.D. dissertation, Royal Institute Technology, Stockholm, Sweden, Mar. 1996.
[10] J. Fuhl, A. Molisch, and E. Bonek, "Unified channel model for mobile radio systems with smart antennas," *Proc. Inst. Elect. Eng.*, vol. 145, pp. 32–41, Feb. 1998.
[11] M. Simon and M.-S. Alouini, "A unified approach to the performance analysis of digital communication over generalized fading channels," *Proc. IEEE*, pp. 1860–1877, Sept. 1998.
[12] E. Al-Hussaini and Al-Bassiouni, "Performance of MRC diversity systems for the detection of signals with Nakagami fading," *IEEE Trans. Commun.*, vol. COM-33, pp. 1315–1319, Dec. 1985.
[13] A. A. Abu-Dayya and N. C. Beaulieu, "Analysis of switched diversity systems on generalized fading channels," *IEEE Trans. Commun.*, vol. 42, pp. 2959–2966, Nov. 1994.
[14] V. Aalo, "Performance of maximal-ratio diversity systems in a correlated Nakagami fading environment," *IEEE Trans. Commun.*, vol. 43, pp. 2360–2369, Aug. 1995.
[15] P. Lombardo, D. Fedele, and M. M. Rao, "MRC performance for binary signals in Nakagami fading with general branch correlation," *IEEE Trans. Commun.*, vol. 47, pp. 44–52, Jan. 1999.
[16] Q. T. Zhang, "Maximal-ratio combining over Nakagami fading channels with an arbitrary branch covariance matrix," *IEEE Trans. Veh. Technol.*, vol. 48, pp. 1141–1150, July 1999.
[17] P. R. Krishnaiah and M. M. Rao, "Remarks on the multivariate gamma distribution," *Amer. Math. Monthly*, vol. 68, pp. 342–346, Apr. 1961.
[18] M. Schwartz, W. R. Bennett, and S. Stein, *Communication Systems and Techniques*. New York: McGraw-Hill, 1966.

[19] J. G. Proakis, *Digital Communications*, Third ed. New York: McGraw-Hill, 1995.
[20] A. Papoulis, *Probability Random Variables, and Stochastic Processes*. New York: McGraw-Hill, 1965.
[21] T. W. Anderson, *Introduction to Multivariate Statistical Analysis*. New York: Wiley, 1958.
[22] N. L. Johnson, S. Kotz, and N. Balakrishnan, *Continuous Univariate Distributions*. New York: Wiley, 1994, vol. 1.
[23] H. Cramer, *Mathematical Methods of Statistics*. Princeton, NJ: Princeton Univ. Press, 1946.
[24] *Handbook of Mathematical Functions*, M. Abramowitz and I. A. Stegun, Eds., National Bureau of Standards, Washington, DC, 1972.
[25] J. D. Kraus, *Antennas*, 2nd ed. New York: McGraw-Hill, 1988.
[26] I. J. Gupta and A. A. Ksienski, "Effect of mutual coupling on the performance of adaptive arrays," *IEEE Trans. Antennas Propagat.*, vol. AP-31, pp. 785–791, Sept. 1983.
[27] R. H. Clarke, "A statistical theory of mobile radio reception," *Bell Syst. Tech. J.*, vol. 47, pp. 957–1000, July–Aug. 1968.
[28] P. J. Crepeau, "Uncoded and coded performance of MFSK and DPSK in Nakagami fading channels," *IEEE Trans. Commun.*, vol. 40, pp. 487–493, Mar. 1992.

Jianxia Luo (S'97) received the B.Sc. degree in electronics and information systems from NanKai University, Tianjin, China, and the M.Eng. degree in electrical engineering from Jiaotong University, Shanghai, China, in 1992 and 1995, respectively. She is currently pursuing the Ph.D. degree at the University of California, San Diego.

Since 1996, she has been with Hughes Network Systems, Inc., San Diego, CA, where she was engaged in the development of an enhanced ACELP vocoder for fixed-wireless terminal and satellite-GSM dual-mode handheld terminal. Her research interests include digital signal processing in communications, adaptive array processing, diversity reception in fading channels, and propagation aspects of mobile radio systems.

James R. Zeidler (M'76–SM'84–F'94) received the Ph.D. degree in physics from the University of Nebraska, Lincoln, in 1972.

Since 1974, he has been a Scientist at the Space and Naval Warfare Systems Center, San Diego, CA. Since 1988, he has also been an Adjunct Professor of electrical and computer engineering at the University of California, San Diego. During this period, he has conducted research on communications systems, sonar and communications signal processing, communications signals exploitation, undersea surveillance, array processing, underwater acoustic communications, infrared image processing, and electronic devices. He was also a Technical Advisor in the Office of the Assistant Secretary of the Navy (Research, Engineering and Systems), Washington, DC, from 1983 to 1984. He is a Member of the Editorial Board of the *Journal of the Franklin Institute*.

Dr. Zeidler was an Associate Editor of the IEEE TRANSACTIONS ON SIGNAL PROCESSING from 1991 to 1994. He received the Lauritsen–Bennett award for achievement in science in 2000 and the Navy Meritorious Civilian Service Award in 1991. He was a Corecipient of the award for best unclassified paper at the IEEE Military Communications Conference in 1995.

Stephen McLaughlin (M'88) was born in Clydebank, Scotland, U.K., in 1960. He received the B.Sc. degree in electronics and electrical engineering from the University of Glasgow, Scotland, in 1981 and the Ph.D. degree from the University of Edinburgh, Scotland, in 1989.

From 1981 to 1984, he was a Development Engineer with Barr & Stroud Ltd., Glasgow, involved in the design and simulation of integrated thermal imaging and fire control systems. From 1984 to 1986, he worked on the design and development of high-frequency data communication systems with MEL Ltd. In 1986, he joined the Department of Electrical Engineering, University of Edinburgh, as a Research Associate, where he studied the performance of linear adaptive algorithms in high noise and nonstationary environments. In 1988, he joined the teaching staff at Edinburgh, and in 1991, he was awarded a Royal Society University Research Fellowship to study nonlinear signal processing techniques. His research interests lie in the fields of adaptive signal processing and nonlinear dynamical systems theory and their applications to biomedical and communication systems.

Dr. McLaughlin is an associate member of the Institution of Electrical Engineers.